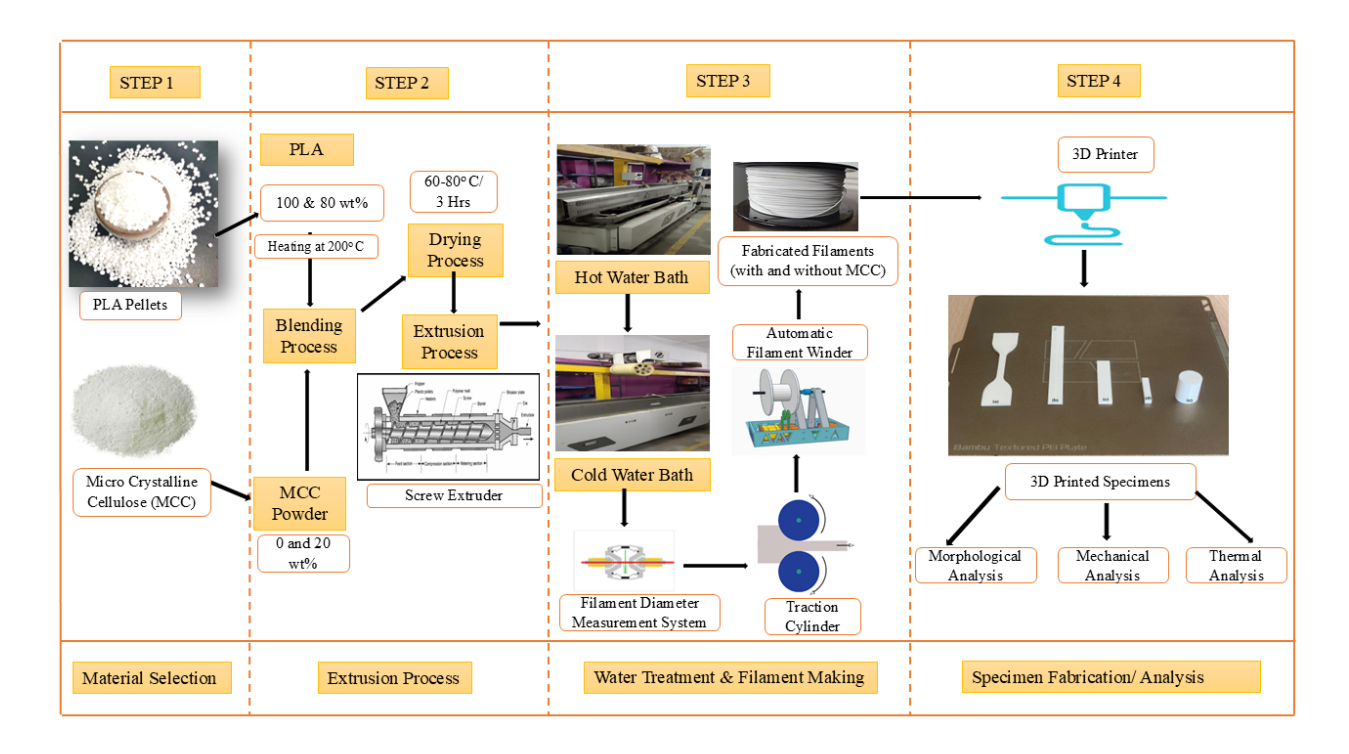
# 3D-Printed Green Biocomposites from Poly(lactic acid) and Pine Wood-derived Microcrystalline Cellulose: Characterization and Properties

Selwin Maria Sekar,<sup>a</sup> Rajini Nagarajan,<sup>a,\*</sup> Ponsuriyaprakash Selvakumar,<sup>b</sup> Nadir Ayrilmis,<sup>c</sup> Kumar Krishnan,<sup>d</sup> Faruq Mohammad,<sup>e</sup> Hamad A. Al-Lohedan,<sup>e</sup> and Sikiru O. Ismail <sup>f</sup>

\*Corresponding author: rajiniklu@gmail.com

DOI: 10.15376/biores.20.4.8473-8492

## **GRAPHICAL ABSTRACT**



# 3D-Printed Green Biocomposites from Poly(lactic acid) and Pine Wood-derived Microcrystalline Cellulose: Characterization and Properties

Selwin Maria Sekar,<sup>a</sup> Rajini Nagarajan,<sup>a,\*</sup> Ponsuriyaprakash Selvakumar,<sup>b</sup> Nadir Ayrilmis,<sup>c</sup> Kumar Krishnan,<sup>d</sup> Faruq Mohammad,<sup>e</sup> Hamad A. Al-Lohedan,<sup>e</sup> and Sikiru O. Ismail <sup>f</sup>

The increasing demand for sustainable and high-performance materials has prompted research into biocomposites as eco-friendly alternatives to traditional plastics. Poly(lactic acid) (PLA), which is widely used, often lacks the mechanical and thermal stability required for advanced applications. This limitation can be overcome by reinforcing PLA with microcrystalline cellulose (MCC), a renewable and abundant resource. While existing PLA composites have shown promise, the uniform dispersion and interfacial bonding of reinforcements remain challenges. To bridge this gap, an optimal 80:20 wt% PLA/MCC ratio was identified and processed into filament using a single-screw extruder, followed by 3D printing via fused filament fabrication (FFF). The composite's properties were evaluated through mechanical, thermal, and morphological analyses. Results revealed significant enhancements: tensile strength increased by 30%, flexural strength by 22.3%, impact strength by 78.9%, and compressive strength by 21.3%, compared to neat PLA. Thermogravimetric analysis showed improved thermal stability, with reduced weight loss at elevated temperatures. This research demonstrates that the integration of MCC into PLA not only improves mechanical and thermal properties but also offers an environmentally sustainable solution for engineering applications. The findings highlight the potential of PLA/MCC composites for industries requiring lightweight, durable, and eco-conscious materials, including automotive and biomedical sectors.

DOI: 10.15376/biores.20.4.8473-8492

Keywords: Polylactic acid; Microcrystalline cellulose; Fused filament fabrication morphology; Screw extruder; 3D printing; Renewable

Contact information: a: Department of Mechanical Engineering, Kalasalingam Academy of Research and Education, Krishnankoil, Tamilnadu 626 126 India; b: Department of Mechanical Engineering, Mangayarkarasi College of Engineering, Madurai, Tamilnadu, India; c: Department of Wood Mechanics and Technology, Faculty of Forestry, Istanbul University – Cerrahpasa, Bahcekoy, Sariyer, 34473, Istanbul, Turkey; d: INTI International University, Persiaran Perdana BBN, 71800 Nilai, Negeri Sembilan, Malaysia; e: Department of Chemistry, College of Science, King Saud University, P.O. Box 2455, Riyadh, 11451, Kingdom of Saudi Arabia; f: Department of Engineering, Centre for Engineering Research, School of Physics, Engineering and Computer Science, University of Hertfordshire, Hatfield AL10 9AB, England, United Kingdom; \*Corresponding author:rajiniklu@gmail.com

# INTRODUCTION

Additive manufacturing(AM) has revolutionized production by directly transforming 3D models into finished products by eliminating complex tooling such as jigs

and enabling intricate designs (Kruth *et al.* 1998). This promotes sustainability through minimal waste generation and aligns with lean manufacturing principles (Guo and Leu 2013). Since AM's ability multiple components are combined into unified structures, coupled with topology optimization (Huang *et al.* 2012), it is possible to create lightweight, efficient products that maximize functionality while minimizing material and energy use (Wang *et al.* 2016; Lee *et al.* 2017).

Recent studies have focused on eco-friendly materials to mitigate the environmental impact of waste plastics, particularly for structural applications involving the automotive manufacturing industries (Ngo et al. 2018). Sustainable fillers have emerged as viable substitutes for creating environmentally friendly polymer composites, though challenges such as handling and flexibility persist. Nonetheless, these challenges can be addressed by utilizing bonding agents, supplementary substances, or chemical modifications (Sachin et al. 2020). Biomaterials have been successfully integrated into matrices such as poly(lactic acid) (PLA), polypropylene (PP), polyethylene (PE), and acrylonitrile butadiene styrene plastic (ABS) through chemical treatments and additives that improve mechanical properties (Shao et al. 2018). As the 3D printing market for these composites expands, material quality is expected to improve. Future research should prioritize biodegradable options such as PLA and other strong materials such as polycarbonate (PC), ABS, and medical-grade alternatives, while also optimizing biomaterial processing (Lamm et al. 2020; Lupuleasa et al. 2018; Ismail et al. 2023).

PLA is a thermoplastic that can be derived from renewable sources such as corn and sugarcane, making it environmentally friendly and biocompatible (Velu *et al.* 2019; Bassani *et al.* 2019). It has high tensile strength and stiffness, making it suitable for stability-critical applications such as biomedical use, and its byproducts are safe for humans and the environment (Kalsoom *et al.* 2016; Farah *et al.* 2016). PLA production is more energy efficient than petroleum-based polymers because its key component, lactic acid, is derived from renewable sugars (Alzahmi *et al.* 2022), which contributes to its environmental sustainability (Blanco 2020; DeStefano *et al.* 2020).

3D printing filament production can be carried out with inclusion of sustainable materials such as microcrystalline cellulose (MCC), which is derived from cellulose by removing amorphous parts, resulting in rod-like fibrils with high strength and crystallinity (Estakhrianhaghighi *et al.* 2020). MCC significantly enhances composite properties, reducing weight and cost while improving thermal and mechanical performance (Crews *et al.* 2016; Fonseca *et al.* 2021). Prepared from sources such as delignified pinewood, MCC features high alpha-cellulose content, fine particle size (109 μm), porosity (76%), and low density (0.36 g/cm³), making it suitable for applications in biocomposites, food, cosmetics, and pharmaceuticals (Selwin *et al.* 2024). When optimally blended with PLA, MCC can improve filament properties (Cavallo *et al.* 2020), including enhanced mechanical strength (Singhvi *et al.* 2019), thermal stability, and resistance to weight loss at lower temperatures (Bhasney *et al.* 2020; Selwin *et al.* 2024).

Fuse filament fabrication (FFF)-based 3D printing is popular because it is inexpensive, quick, and simple to use, requires little post-processing, and has adjustable settings for strength and functionality. Unlike computerized numerical control (CNC) milling, it requires fewer adjustments, though interlayer distortion can weaken parts (Lupuleasa *et al.* 2018). However, FFF has limitations, such as weaker parts, visible layer textures, rough finishes, and limited material choices (Velu *et al.* 2019; Blanco 2020). To address these problems, fiber-reinforced composites have been developed, which improve

the strength of FFF-printed parts. Despite their potential, challenges such as fibre orientation, bonding, and voids remain to be addressed (Ankit *et al.* 2019; Wang *et al.* 2016). This study contributes to these efforts by developing hybrid composite filaments for producing specimens with improved mechanical properties. In addition, investigating the thermal stability of PLA with the addition of MCC is another objective of this study. Studies in the literature mainly have investigated the mechanical and thermal properties of biocomposites printed on 3D printers from filaments produced by adding low amounts of the MCC to the PLA (Qu *et al.* 2010).

This study explores the development of hybrid composite filaments by incorporating higher proportions of microcrystalline cellulose (MCC) into PLA, surpassing the focus of prior research on low MCC content. It provides a comprehensive analysis of the morphological, mechanical, and thermal properties of these biocomposites, aiming to enhance their performance for 3D printing applications. By addressing the effects of higher MCC content, the study advances material optimization for improved mechanical strength, thermal stability, and sustainability, contributing to the eco-friendly evolution of FFF-based 3D printing technologies.

#### **EXPERIMENTAL**

# Polylactic Acid (PLA)

Commercial PLA in form of pellets was obtained from Greendot Biopak company in Ahmedabad, Gujarat, India. The physical and mechanical properties of the PLA are shown in Table 1.

Properties	Values
Density (g/cm <sup>3</sup> )	1.24
Tensile strength (MPa)	60
Flexural strength (MPa)	108
Elongation (%)	9
Young's modulus (MPa)	3100
Shore D hardness (Sh D)	85
Melting temperature (°C)	145-160
Glass transition temperature (°C)	56-64

**Table 1.** Properties of PLA Pellets (Estakhrianhaghighiet al. 2020)

# Microcrystalline Cellulose (MCC)

The source material for preparing the MCC was softwood pulp that had been bleached and had fluffy white fibers (Krapez *et al.* 2024). The ideal type of  $\alpha$ -cellulose for the formation of MCC is abundant in these fibres. Figure 1 shows the isolation process. The MCC is a widely used and adaptable material with applications in food, cosmetics and pharmaceuticals, making it an excellent option as a biocomposite with lower weight and cost (Selwin *et al.* 2024). Due to its high concentration of alpha cellulose, pine softwood was used as the main source of the wood pulp from which it was made.

The microstructure of the cellulose powder examined by FESEM is shown in Fig. 2, where cross-linked fibres are visible. Due to its special properties, this natural wood powder has a tiny particle size of 109  $\mu$ m, a high porosity of 76% and a low weight or density of 1.4 g/cm<sup>3</sup>.

#### **Isolation Process of MCC**

The MCC is typically prepared from lignocellulosic biomass through a series of chemical treatments involving acids, alkalis, and bleaching agents. The conversion of wood pulp to MCC was carried out in several steps, mechanical or chemical pulping to separate the cellulose fibres, followed by purifying bleaching. The amorphous parts of the cellulose were then broken down and the crystallinity increased by acid hydrolysis (Raharjo *et al.* 2023). To prevent degradation, the material was then carefully cleaned and neutralized. Finally, the cellulose fibres were broken down into tiny, high surface area crystals by mechanical refinement. The process culminated in the production of a white, free-flowing MCC powder by drying methods such as spray drying (Krapez Tomec *et al.* 2024). According to the chemical composition study, the prepared MCC consisted of 41.7 wt%  $\alpha$ -cellulose, 19.5 wt% hemicellulose, 17.1 wt% lignin, 4.3 wt% wax, and 7.3 wt% ash. After the ethanol-toluene treatment, the extractives content of the fibres was completely eliminated.

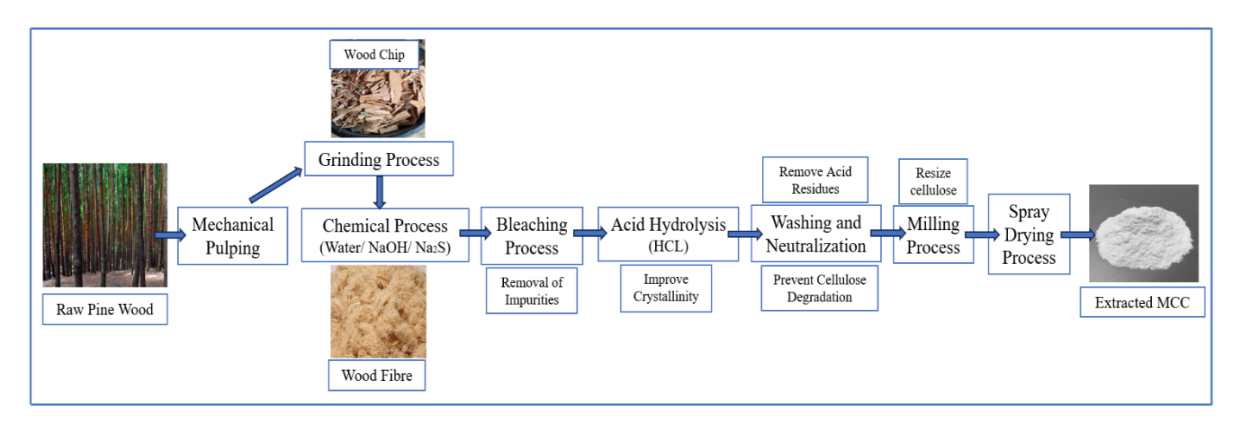


Fig. 1. The MCC isolation process

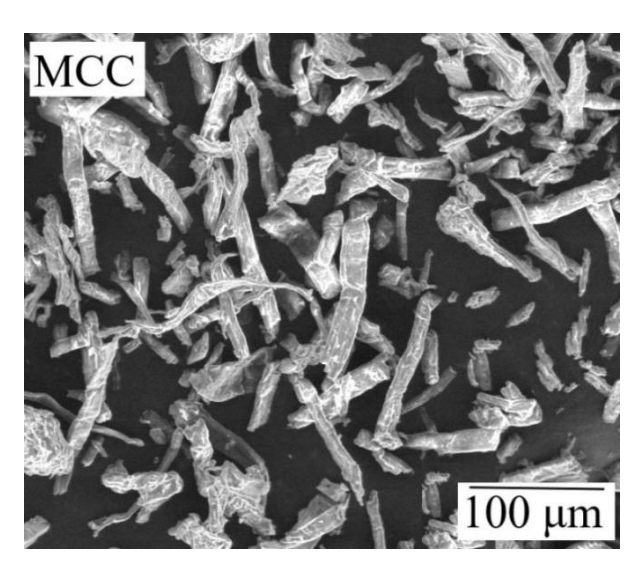


Fig. 2. Microstructure of the MCC

# Preparation of PLA/ MCC Filament Composites

A composite material consisting of 80 wt% PLA and 20 wt% cellulose was selected for filament (wire) production, tailored for use with the FFF 3D printing machine. The

filament extruder machine (FLD-45 3D, Zhangjiagang Friend Machinery Co., Ltd, China), capable of producing 15-20 Kg/h, was utilized to manufacture filament at Augment 3Di Filament Manufacturer in Coimbatore. The extrusion machine features a hopper, a screw extruder, a heating element, and a feed nozzle, boasting a screw diameter of 35.6 mm, a torque of 125 Nm, and a maximum axial pressure of 150 bar. The 80 wt% PLA matrix was prepared as a slurry by heating to 200 °C, followed by the addition of 20 wt% cellulose reinforcement. This mixture was then blended at a rotor speed of 80 rpm for 10 minutes using a compounding process.

The thermal liquification process of PLA material results in no significant alteration of its existing physical and chemical properties when cooled rapidly. The thin mixture of matrix and reinforcement composite material was introduced into the hopper. The procedure commenced with a screw extruder operating at a screw speed of 600 rpm, which was utilized to convey the composite material into a heating element for semi-liquefaction within a temperature range of 200 to 220°C. The filament produced by the nozzle was thoroughly cooled in the water tank. An initial "warm" bath cooling stage was used to reduce uncontrolled material shrinkage and to maintain surface quality. The process concluded with rapid heat removal from the filament strand by immersion in a cold water bath. Real-time, dual-axis diameter measurement to within 0.8 microns was maintained throughout production.

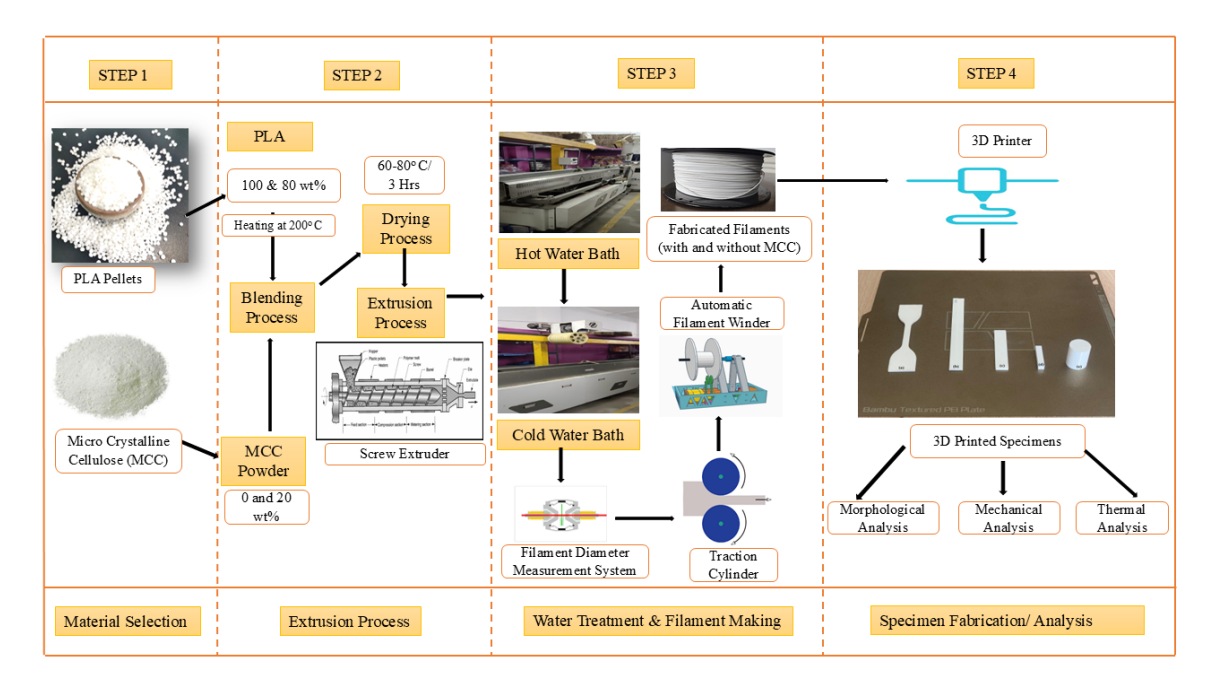


Fig. 3. Methodology of filament preparation and 3D printing of the test specimens

The fabricated filament was measured for the diameter of 1.75 mm using filament diameter measurement system. The semi-molten mixture was then squeezed through a small nozzle with a diameter of 1.75mm, which is the standard size for FFF 3D printer filament (Arumaiselvan *et al.* 2024). The fabricated filament after checking the diameter was sent between a pair of rollers. The purpose of this step was to produce the filament with a smooth surface, ensuring that there was no change in the filament diameter. The filament was then wound into a spool using an automatic filament winder. The wound filament is shown in Fig. 4.

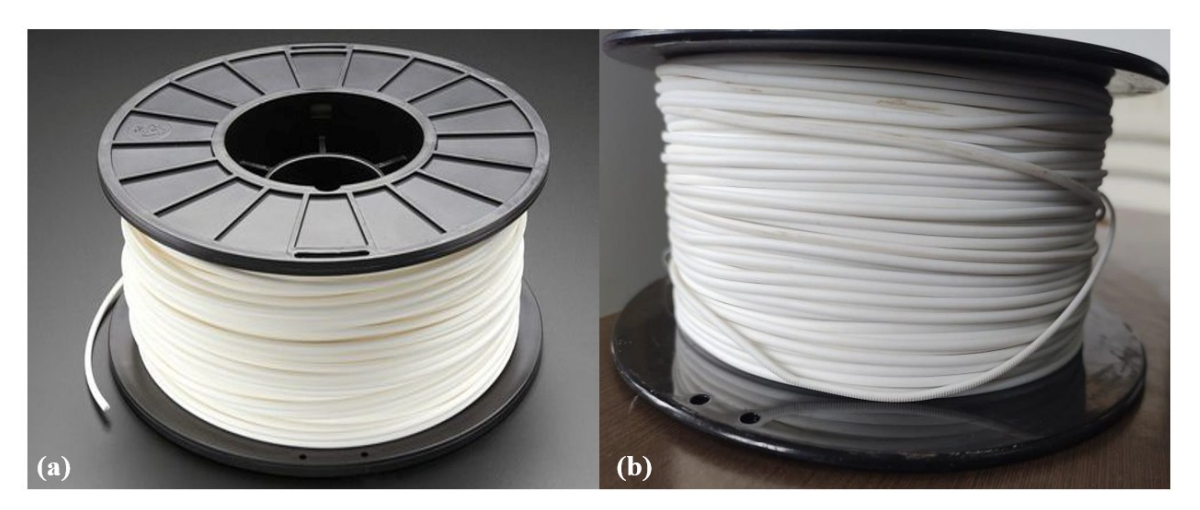


Fig. 4. Filament fabricated (a). PLA/MCC (100:0 wt%) (b). PLA/MCC (80:20 wt%)

# Slicing Process Using Bambu Studio Software

Bambu studio (v1.9.5) was used for both 3D modelling and the physical creation process. It is a slicing software that imports the 3D model and prepares it for printing across various machines by converting the model's geometry into instructions that are understandable by a printer (known as slicing) (Fig.5). The parameters for the slicing process were defined in terms of layer thickness, infill density, and support structures, all of which significantly impact the final quality of the 3D printing including such as strength and printing time. As per ASTM standards, the specimens for the tensile, flexural, impact, hardness, and compression were designed using solid works software (SOLIDWORK 2024).

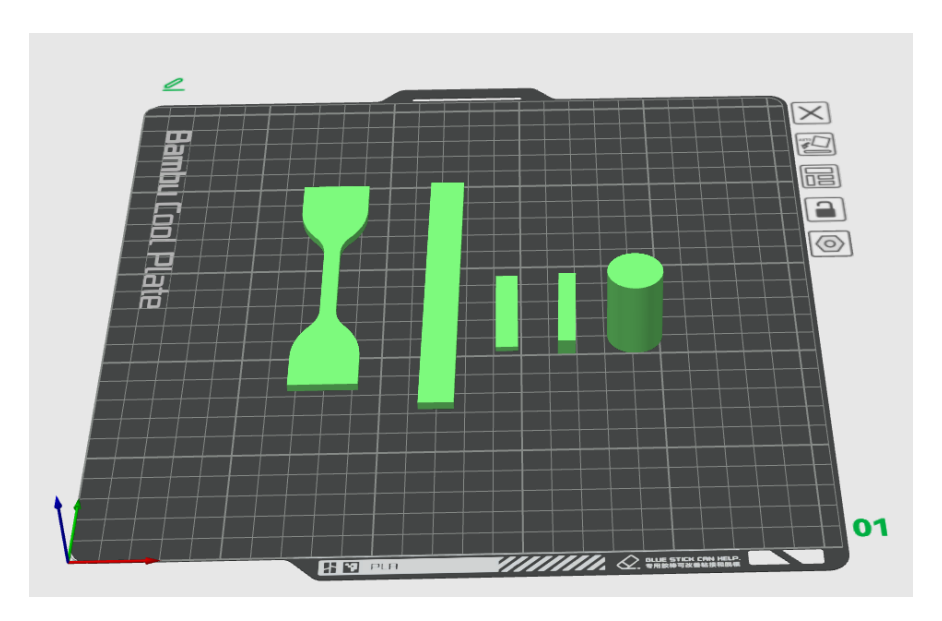


Fig. 5. Slicing process using Bambu studio software

The test specimens were fabricated from the developed PLA/cellulose composite filament using a Bambu Labs X1E printer (Shenzhen, China) (Fig. 6), which works with an extrusion-based FFF process to fabricate models. It has a glass build platform measuring (256 mm by 256 mm). Its nozzle is able to move precisely in three directions (X, Y, and

Z). The nozzle has a diameter of 0.4 mm, and the nozzle temperature ranged from 190 to 260 °C. The machine parameters for printing are as shown in Table 2.

Nozzle diameter (mm)	0.4
Printing speed (mm/s)	250
Bed temperature (°C)	60
Nozzle temperature (°C)	220
Infill pattern	Cube
Infill density (%)	100
Layer height (mm)	0.2
Raster angle (°)	0

After simulating and analyzing the design using computer-aided design (CAD) software, the generated toolpath data (G-code) was uploaded from Bambu Studio software to the Bambu Labs X1E 3D printer. The printing process then begins with the printer loading and extruding a composite filament. The specimen fabrication steps are shown in Fig. 7. The printed components were removed from the printer bed, and the support structures were removed after printing. The printed surfaces were smoothed with acetone solvent.

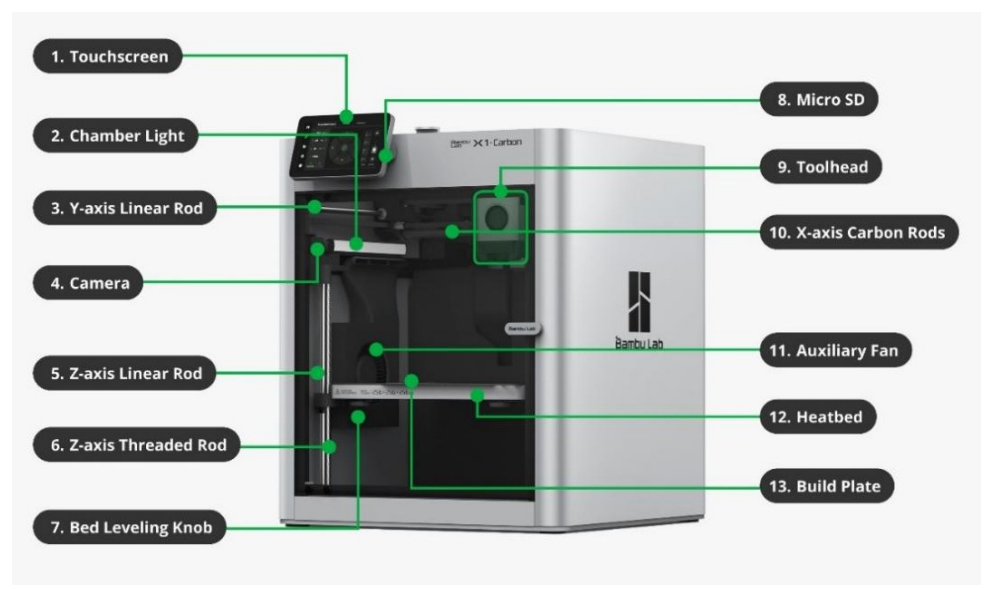


Fig. 6. Bambu labs X1E FFF printer specifications

# **Determination of Mechanical Properties**

Tensile test

A universal testing machine (Generic Tensile Stress vs. Strain H10KL/150 = 10000 N, Instron, Norwood, Massachusetts, USA) was used to conduct the tensile tests on Cellulose/PLA composites at room temperature in compliance with the ASTM D638-14 standard (2022).

Flexural test

At room temperature, the 3-point flexural tests of PLA/cellulose composites were conducted using the Generic Flexure 3PT, which is in line with the ASTM D790 standard

universal testing equipment (H10KL/150 = 10000 N, Instron, Norwood, Massachusetts, USA) (Wang *et al.* 2024).

## Impact test

In order to determine the maximum amount of energy that each PLA matrix and cellulose-reinforced composite material could absorb, the Izod impact test was carried out. An impact testing machine of the pendulum kind (made by Tinius Olsen Pvt. Ltd, Horsham, Pennsylvania, USA) was used to conduct the test. The specimens were measured in accordance with the ASTM D256-07 testing standard. The manufactured specimens' average impact strengths were determined using the following parameters: impact velocity 3.55 m/s, distance 615 mm, and impact energy 12.5 J.

#### Hardness test

The polymer-based composites were tested for hardness according to the Shore Durometer hardness D-scale (ASTM D2240-15 2021). A mechanical shore (D-scale) Durometer hardness machine (Fasne test equipment Pvt. Ltd, Sangli, Maharashtra, India) was used to measure the hardness of the PMC samples that were manufactured. The temperature at which all mechanical hardness assessments were conducted was 25°C.

## Compression test

Composite materials with cellulose reinforcement and a PLA matrix were tested for compression strength using a universal testing equipment (Generic compression, H10KL/150 = 10000 N, Instron, Norwood, Massachusetts, USA) in compliance with ASTM D695 standard. The load cell delivered a 50 kN force at a 5 mm/min cross-head speed to determine the ultimate compression strength (UCS) of all six manufactured specimens.

#### *X-ray diffraction (XRD) analysis*

XRD analysis using an Advanced Panalytical Xpert Pro diffractometer(Malvern Panalytical Ltd, Netherlands)was conducted to examine the crystalline structure of a composite material. This composite consisted of an 80 wt% PLA matrix reinforced with 20 wt% microcrystalline cellulose (MCC). The diffraction patterns were collected over a  $2\theta$  range from  $10^{\circ}$  to  $80^{\circ}$  at a scan rate of  $4^{\circ}$ /min.

#### Morphology of fracture surface

Field Emission Scanning Electron Microscopy (FESEM with EDAX, Quanta FEG-250 SEM instrument, Thermo Fisher Scientific, Waltham, Massachusetts, USA) was employed to examine the topography of the broken surfaces of Cellulose/PLA composites. Prior to FESEM perceptions, all examples were consistently covered for 3 min by a sputtering technique. Here it is to be noted that the FEG column in Quanta 250 permits the beam to be decelerated, thereby achieving a resolution of 1.4 nm even at 1 kV electron landing Voltage.

## Thermogravimetric analysis (TGA)

Thermogravimetric analysis was carried out on specimens (10 to 15 mg) in a nitrogen environment after oven drying (TGA Q500 model, TA Instruments private limited, New Castle, Delaware, USA.) specimens were heated at a rate of 10°C per minute from an initial temperature of 30°C to a final temperature of 900 °C. The heat flow

associated with the thermal events in the specimen relative to an inert reference was measured (Kowalczyk et al. 2011).

Fourier transform infrared spectroscopy (FTIR) analysis

A Thermo Nicolet 380 FTIR spectrophotometer (Thermo Fisher Scientific, Waltham, United States) was used to investigate solvent-induced chemical changes in PLA/cellulose composites that had been manufactured in accordance with ASTM E168 standard. A tiny sample of the PLA/cellulose composite was cut with a typical thickness of 200 µm. The peaks that indicated the presence of PLA/cellulose in every sample were observed in the 4000 to 400 cm<sup>-1</sup> wavelength range. Featuring a DLaTGS detector (Laser Components USA Inc, Bedford, United States) with a 0.5 cm<sup>-1</sup> resolution and a basic setup of 0.01 cm<sup>-1</sup>wave number accuracy and 2000: 1 ppm for a 1-minute scan. This FTIR spectrometer was custom-built.

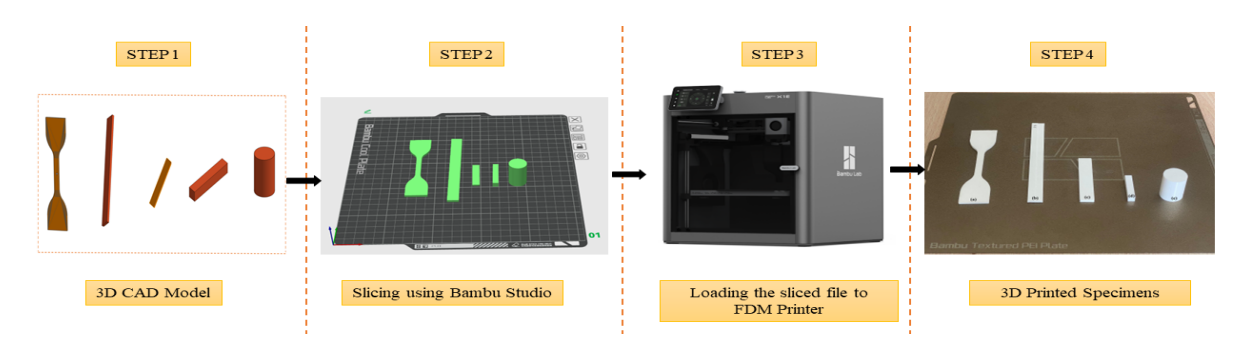
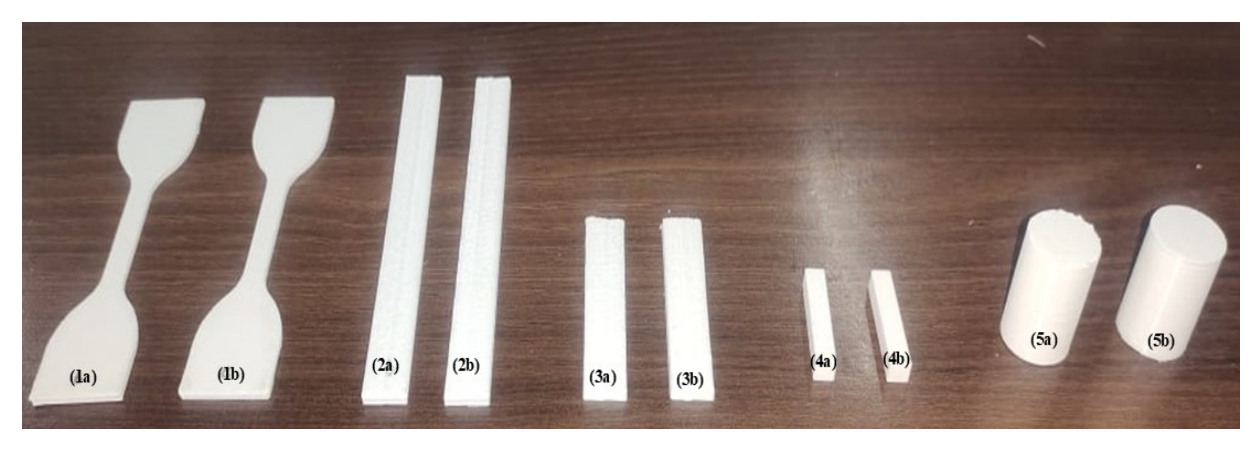


Fig. 7. Fabrication of 3D printed specimens



**Fig. 8.** The 3D printed test specimens. 1.(a) Tensile specimen of pure PLA (b). Tensile specimen of 80:20 wt% PLA/MCC composite.2. (a) Flexural specimen of pure PLA(b) Flexural specimen of 80:20 wt% PLA/MCC composite.3. (a). Impact specimen of pure PLA. (b) Impact specimen of 80:20 wt% PLA/MCC composite.4. (a). Hardness specimen of pure PLA (b). Hardness specimen of 80:20 wt% PLA/MCC composite.5. (a). Compression specimen of PLA (b). Compression specimen of 80:20 wt% PLA/MCC composite

#### **RESULTS AND DISCUSSION**

# **PLA/MCC Filament Composites**

It was found that 80:20 wt% of PLA/MCC composites gave the best result in all aspects. Accordingly, that combination was chosen for filament fabrication. With this result, further analysis to evaluate the filament composite was done using the composition of 80:20 wt% of PLA/MCC. A filament extruder (FLD-45 3D, Zhangjiagang Friend Machinery Co., Ltd, China) was used to create the filament. The filament was extruded into spools of wire (Whyman *et al.* 2018). The filament extruder has several parts, namely a hopper to feed the material, a special type of extruder with a screw (single screw extruder), a heating element to melt the material, and a nozzle that pushes the melted plastic out. The screw diameter is 35.6 mm, with the ability to generate 125 Nm torque, and can handle pressure up to 150 bar (Ponsuriyaprakash *et al.* 2023).

The mixed PLA/MCC pellets were hygroscopic, meaning that they absorbed moisture from the air, which can deform or degrade the plastic. Therefore, removing any moisture from the pellets *via* the drying method is necessary to ensure the production of quality filament. The filament was composed of 80 wt.% polylactic acid (PLA) for a strong base and 20 wt.% cellulose reinforcement for the added properties, as displayed in Fig.8.

# X-ray Diffraction (XRD) Analysis

The XRD analysis was carried out to verify the addition of MCC reinforcement within the PLA matrix composite. The XRD patterns of Pure PLA, pristine PLA, and MCC filler for comparisonare presented in Fig. 9.

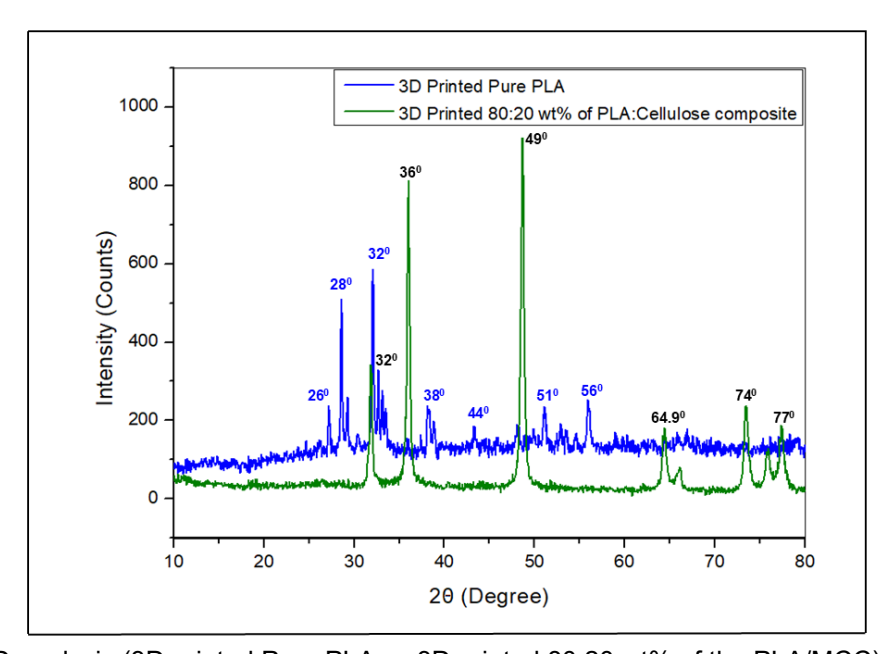


Fig. 9. XRD analysis (3D printed Pure PLA vs 3D printed 80:20 wt% of the PLA/MCC)

Distinct peaks at  $2\theta = 32^{\circ}$ ,  $36^{\circ}$ ,  $49^{\circ}$ ,  $64.9^{\circ}$ ,  $74^{\circ}$ , and  $77^{\circ}$  in the PLA/MCC composite spectrum confirmed the presence of the MCC, as evidenced by its intensity. Similarly, distinct peaks at  $2\theta = 26^{\circ}$ ,  $28^{\circ}$ ,  $32^{\circ}$ ,  $38^{\circ}$ ,  $44^{\circ}$ ,  $51^{\circ}$ , and  $56^{\circ}$  indicated the crystalline nature of pure PLA (Ali*et al.* 2022). The strongest peaks corresponded to the PLA matrix, while the weakest peaks corresponded to the MCC reinforcement.

# Fourier Transform Infrared Spectroscopy (FTIR) Analysis

FTIR was employed to assess the presence and distribution of cellulose within PLA/MCC composites (20 wt% MCC). Characteristic cellulose stretching vibrations were observed in the wavenumber range of 700 to 3400 cm<sup>-1</sup>, with the peak at 1600 cm<sup>-1</sup>. The intensity of these peaks exhibited a positive correlation with increasing MCC content (Fig. 10), suggesting successful dispersion throughout the PLA matrix (Ponsuriyaprakash *et al.* 2020). However, the chemical treatment significantly enhanced the broad peak around 1600 cm<sup>-1</sup> and a corresponding decrease in the intensity of the characteristic cellulose peaks at 700, 1100, 1400, 2250, 2850, and 3400 cm<sup>-1</sup>. This observation suggests a potential reduction in the amount of detectable cellulose, which could be advantageous for improving the mechanical properties of the composite fibers, as high cellulose content can be detrimental (Selwin *et al.* 2024). Furthermore, the complete elimination of the distinct cellulose peaks was observed in some chemically treated specimens.

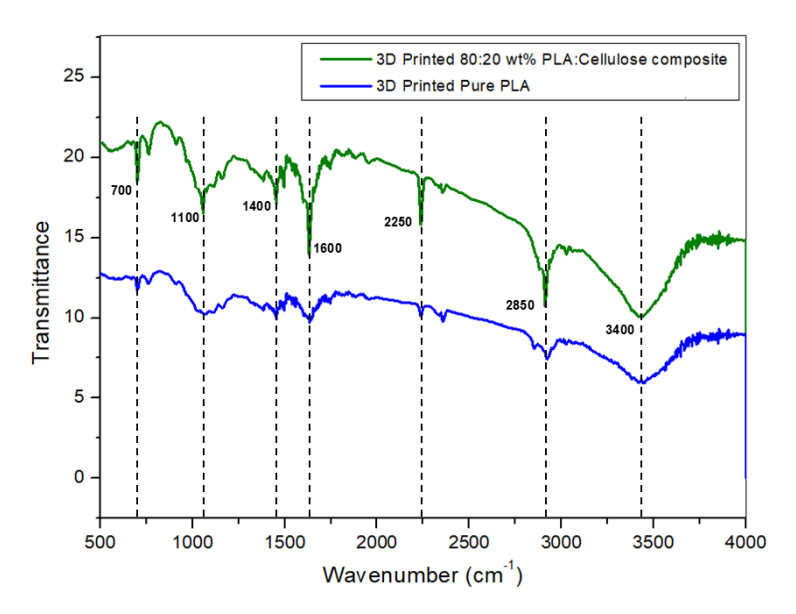


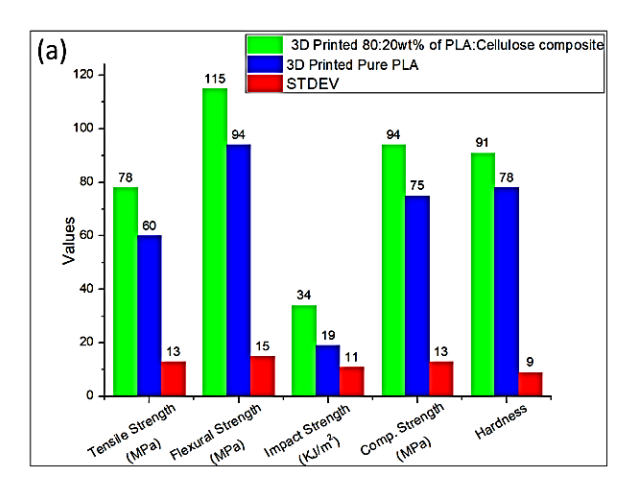
Fig. 10. FTIR analysis (3D printed Pure PLA vs 3D printed 80:20 wt% of the PLA/MCC)

The FTIR results discussed here provide useful insights into the interaction between PLA (polylactic acid) and MCC (microcrystalline cellulose), particularly regarding the dispersion and chemical treatment of cellulose in PLA-MCC composites. The FTIR spectra clearly indicate the presence of cellulose (Ponsuriyaprakash *et al.* 2020) in the composite, especially through characteristic bands within the 700to3400 cm<sup>-1</sup> range, with the peak at 1600 cm<sup>-1</sup> being especially prominent. An intense absorption band was observed near 1600 cm<sup>-1</sup> in the FTIR spectrum of the PLA/MCC composites. While this peak is not typically attributed to cellulose, its sharpness and intensity in the composite samples suggest a possible interaction-induced shift. This phenomenon may be explained by the role of microcrystalline cellulose (MCC) as a nucleating agent, which promotes crystallization of the PLA matrix. The semi-crystalline nature of MCC and its abundant hydroxyl groups facilitate hydrogen bonding with the PLA carbonyl groups, potentially leading to increased molecular ordering. Such interactions can enhance PLA crystallinity, which, in turn, may sharpen and intensify specific IR bands due to altered vibrational environments. Therefore, the pronounced peak near 1600 cm<sup>-1</sup> may not arise directly from MCC but rather from

PLA's enhanced crystallinity and intermolecular interactions between the two components. This hypothesis aligns with similar findings reported in literature where the inclusion of cellulose-based fillers led to spectral shifts and increased structural order in PLA composites (Moon et al. 2011; Yetis et al. 2023). This data supports the hypothesis that cellulose is successfully incorporated into the PLA matrix, and its distribution increases with higher MCC content, as evidenced by the positive correlation between peak intensity and MCC concentration. However, the chemical treatment of MCC seemed to modify the cellulose structure. The enhancement of the broad peak around 1600 cm<sup>-1</sup> and the reduction or elimination of several characteristic cellulose peaks (700, 1100, 1400, 2250, 2850, and 3400 cm<sup>-1</sup>) suggest that the chemical treatment affected the cellulose's molecular structure, potentially reducing its crystallinity or altering its functional groups. This could have important implications for the composite's properties, particularly its mechanical behavior. The reduction in detectable cellulose might improve the mechanical properties of the composite fibers, as the higher cellulose content can sometimes cause brittleness or other detrimental effects on the overall performance of the material. The FTIR results thus provide valuable chemical insights, but the observed changes, especially after chemical treatment, also hint at a deeper modification of cellulose that may not be fully captured through FTIR alone. The decrease in certain peaks could suggest a reduction in cellulose crystallinity or changes in the hydrogen bonding network (Selwin et al. 2024), which could be corroborated with additional analytical techniques such as X-ray diffraction (XRD) or scanning electron microscopy (SEM).

# **Mechanical Properties of 3D Printed Specimens**

Table 4 shows that incorporating 20 wt% MCC into a polymer fiber composite increased its tensile strength compared to pure PLA. This enhancement is attributed to improved bonding between the MCC and the PLA matrix, confirmed by examining the microstructure using FESEM. The FESEM analysis also revealed a homogenous distribution of the MCC particles throughout the PLA matrix.



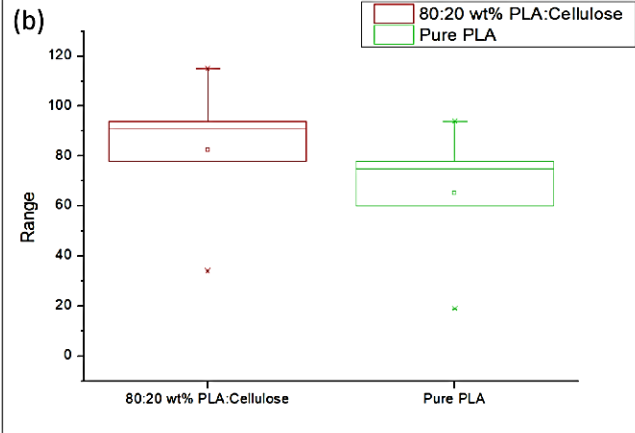


**Fig. 11. (a)** Mechanical behaviour of the pure PLA *vs.* MCC reinforced PLA specimens. (b) Box Plot PLA *vs.* MCC reinforced PLA specimens

Mechanical Behavior	Pure PLA	80 wt% PLA+ 20 wt% MCC
Tensile strength (MPa)	60	78
Flexural strength (MPa)	94	115
Impact strength (kJ/m²)	19	34
Compression strength (MPa)	75	91
Hardness (Shore D)	78	94

Table 4. Mechanical Behavior of the 3D Printed Specimens

A fractography analysis was done to examine the broken surface (fracture) of the composite filament (Fig. 12b). The fractography analysis revealed strong adhesion between the PLA and the MCC particles (Fig. 12c), which improved the bonding performance and allowed for more effective stress transfer throughout the composite, significantly enhancing its resistance to pulling forces (Ponsuriyaprakash *et al.* 2020). The micro images obtained using FESEM provided clear visual evidence of the stronger bonding between the PLA matrix and the MCC filler, along with its uniform distribution within the material. This finding is in accordance with a study done by Selwin *et al.* (2024), where the microscopic analysis showed a uniform distribution of cellulose fibers reinforcement within the PLA matrix, suggesting minimal fiber clumping throughout the composite filament.

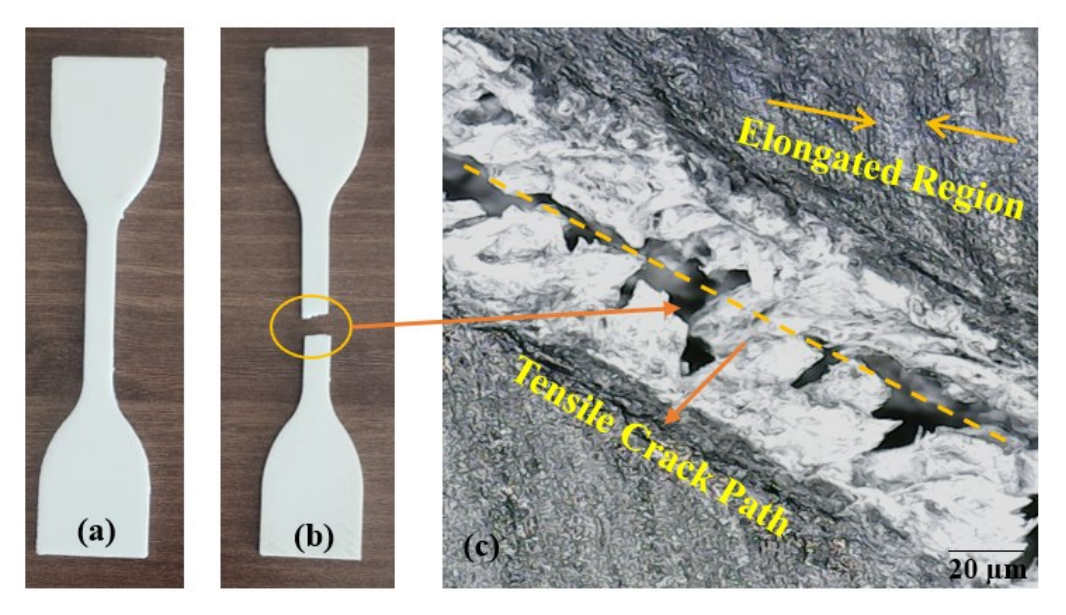


**Fig. 12.** Tensile behaviour. (a).The specimen before the tensile test, (b). The specimen after the tensile test, (c). The FESEM of the tensile crack path

The key to achieving optimal bending strength in PLA/MCC lies in optimizing the MCC filler content, as shown in Fig. 13. In contrast to pure PLA, these composites demonstrated significant improvements in both strength and stiffness due to MCC filler reinforcement. The data show an increase in flexural strength for PLA composites reinforced with 20 wt.% MCC when compared to pure PLA (Fig. 11). These findings provide valuable insights for designing and engineering PLA-based composites with a balance of strength and functionality.

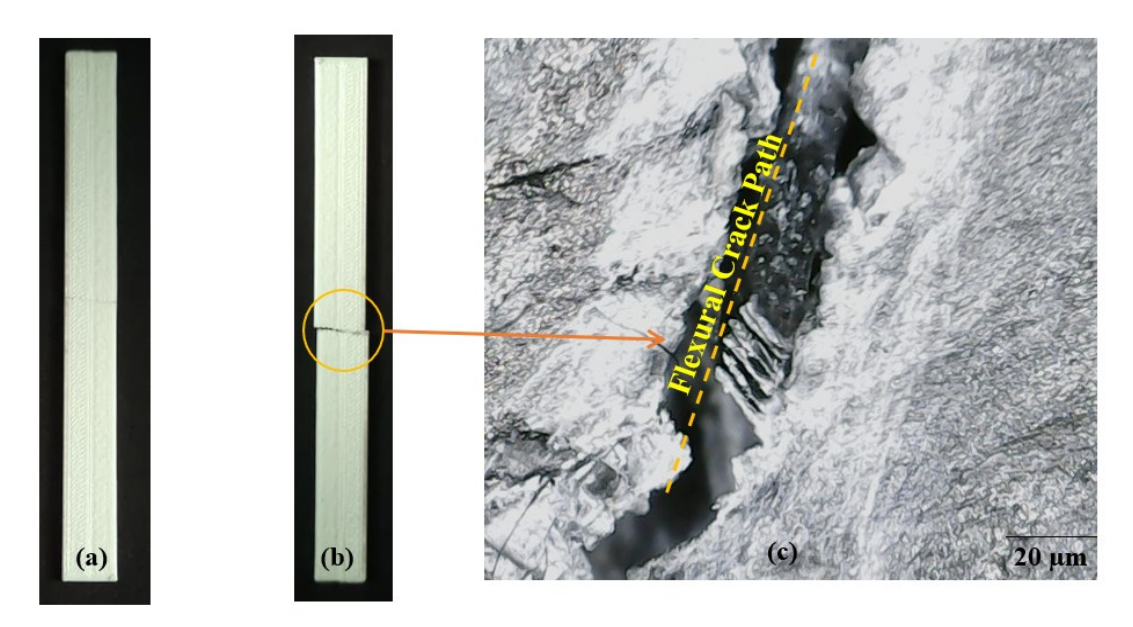


**Fig. 13.** Flexural behaviour. (a). The specimen before the flexural test. (b). The specimen after the flexural test, (c). The FESEM of the flexural crack path

Figure 11 further illustrates that the reinforcement to the PLA by adding 20 wt% MCC significantly increased its impact strength by 78.9%, from to 34 kJ/m². This improvement was mainly attributed to the enhanced interfacial bonding and uniform reinforcement distribution. The uniform distribution of MCC allows the energy to be absorbed energy and prevents cracks from propagating (Ponsuriyaprakash *et al.*2020). The SEM analysis confirmed the enhanced bonding between the PLA and cellulose, leading to a significant improvement in the load transfer from the PLA matrix to the reinforcement MCC in the biocomposites, as shown in Fig. 14.

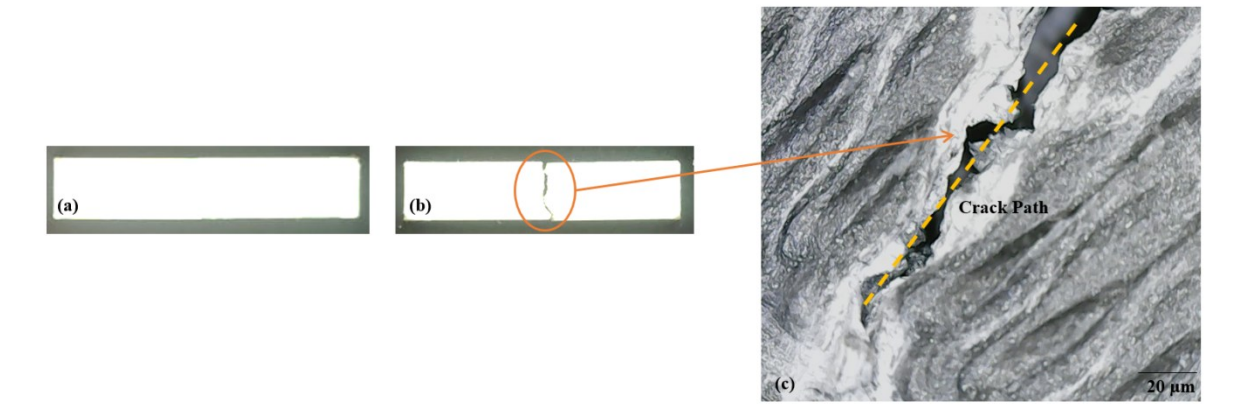


**Fig. 14.** Impact behaviour. (a). The specimen before the impact test; (b). The specimen after the impact test; (c). The FESEM of the impact crack path

The 3D printing process proved to be a powerful tool for creating high-quality biocomposites. This was evident in the hardness data for specimens with the MCC, as presented in Fig. 15. As the cellulose content was increased to 20 wt%, the hardness steadily improved. This trend highlighted two key points: the strengthening effect of cellulose and the success of the 3D printing process in producing biocomposites with

minimal defects (pores, voids) and even fiber distribution. The 80:20 wt% biocomposite stood out with an impressive 20.51% increase in hardness (94 Shore D) compared to the pure PLA (Fig. 11). This achievement showed the potential of 3D printing for manufacturing robust and functional biocomposites and the improvement in compressive strength, indicating a strong bond between cellulose and PLA in the biocomposites. The addition of the MCC significantly enhanced reinforcing properties of the 3D printed specimens with 21.33% increase in the compressive strength (from 75 MPa to 91 MPa) compared to pure PLA.

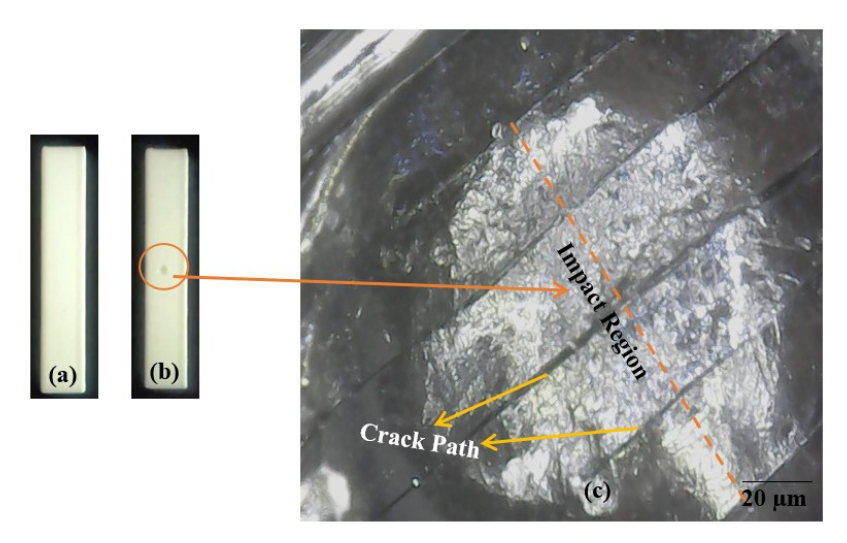


**Fig. 15.** Hardness behaviour. (a). The specimen before the hardness test; (b). The specimen after the hardness test; (c). The FESEM of the hardness crack path

This improvement suggested better interfacial bonding between the PLA and cellulose, facilitating efficient load transfer. Microscopic analysis and FESEM imaging conclusively demonstrated that incorporating the MCC in the optimal ratio significantly enhanced the mechanical properties of the biocomposites (Fig. 16). Such improvement could lead to the development of improved biomaterials with superior qualities for a variety of uses.

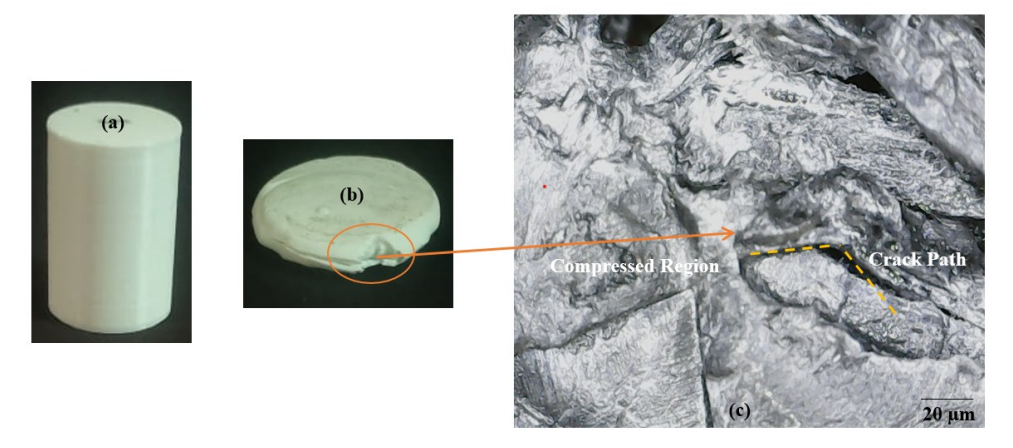


**Fig. 16.** Compression behaviour. (a). The specimen before the compression test; (b). The specimen after the compression test; (c). The FESEM of the compression crack path

# Thermogravimetric Analysis (TGA)

The 80:20 wt% of PLA/MCC composite filament's thermal properties contribute to the printer's accuracy. Figure 17 shows the weight loss data (TGA curve) for the composite specimens. It is apparent that adding the MCC filler to the PLA improved the composite filament's thermal stability.

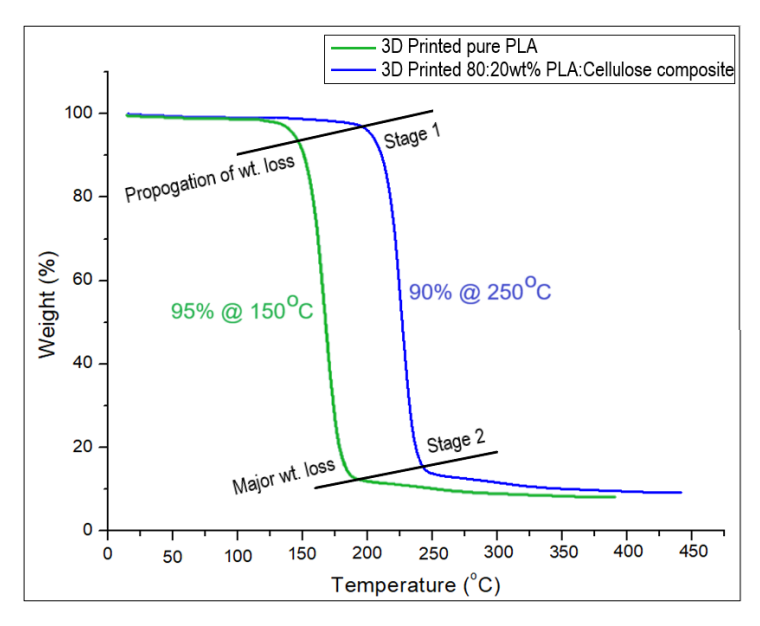


Fig. 17. TGA analysis of the 3D printed 80:20 wt% the PLA/MCC composites

The figure shows that the composite filament with the optimal reinforcement content exhibited weight loss by withstanding the temperature about 250 °C. This suggested that the MCC filler itself started degrading at higher temperatures in stage 2 than in stage 1 because it was shielded by the more thermally stable PLA distributed around it. The enhanced thermal resistivity of the composite filament could be attributed to two factors namely, MCC filler acting as a shield, therefore able to capture harmful free radicals generated during PLA degradation, and the fiber network hindering the escape of volatile degradation products (Selwin *et al.* 2024).

#### CONCLUSIONS

- 1. The 80:20 wt% poly(lactic acid)/microcrystalline cellulose (PLA/MCC)biocomposite showed promising potential for engineering applications based on the data presented.
- 2. The incorporation of MCC into the PLA matrix significantly improved the mechanical properties, including tensile, flexural, impact and compressive strength. This improvement was mainly attributed to the homogeneous dispersion of MCC particles and strong interfacial adhesion within the PLA matrix, as confirmed by X-ray diffraction (XRD) and field emission scanning electron microscopy (FESEM) analysis. Fourier transform infrared (FTIR) spectroscopy further supported the successful integration of MCC and suggested possible chemical modifications that contributed to the improved compatibility.

- 3. In addition to the mechanical properties, the biocomposite exhibited superior thermal stability compared to pure PLA, as evidenced by thermogravimetric analysis (TGA). This thermal stability was crucial for ensuring the long-term performance and durability of the material in various applications.
- 4. Overall, the results of this study suggest that the 80:20 wt% PLA/MCC biocomposite is a viable and promising material for engineering applications that require a combination of high mechanical strength, thermal stability, and sustainability. Further research and development efforts are warranted to explore the full potential of this material in specific applications and to address any potential limitations or challenges.

### **ACKNOWLEDGEMENT**

The authors acknowledge the funding from the Ongoing Research Funding Program (ORF-2025-355), King Saud University, Riyadh, Saudi Arabia.

#### REFERENCES CITED

- Ali, A., Chiang, Y. W., and Santos, R. M. (2022). "X-ray diffraction techniques for mineral characterization: A review for engineers of the fundamentals, applications, and research directions," *Minerals* 12(2), article 205. DOI: 10.3390/min12020205
- Alzahmi, S., Alhammadi, S. Y., ElHassan, A., and Ahmed, W. (2022). "Carbon fiber/PLA recycled composite," *Polymers* 14(11), article 2194. DOI: 10.3390/polym14112194
- Ankit, G., Seymur, H., and Ismail, F. (2019). "Processing and characterization of 3D-printed polymer matrix composites reinforced with discontinuous fibers" *Solid Freeform Fabrication 2019: Proceedings of the 30<sup>th</sup> Annual International Solid Freeform Fabrication Symposium An Additive Manufacturing Conference*, 1054.
- Arumaiselvan, U., Kalimuthu, M., Nagarajan, R., Mohan, M., Ismail, S. O., Mohammad, F., Al-Lohedan, H. A., and Krishnan, K. (2024). "Mechanical, physical and thermal properties of polylactic acid filament composite reinforced with newly isolated Cryptostegia grandiflora fiber," *BioResources* 19(2), 3740-3754.DOI: 10.15376/biores.19.2.3740-3754
- ASTM D256 (2023). "Standard test methods for determining the Izod pendulum impact resistance of plastics," *ASTM International*, West Conshohocken, PA, USA.
- ASTM D638-14 (2022). "Standard test method for tensile properties of plastics," *ASTM International*, West Conshohocken, PA, USA.
- ASTM D695-23 (2023). "Standard test method for compressive properties of rigid plastics," *ASTM International*, West Conshohocken, PA, USA.
- ASTM D790 (2017). "Standard test methods for flexural properties of unreinforced and reinforced plastics and electrical insulating materials," *ASTM International*, West Conshohocken, PA, USA.
- ASTM D2240-15 (2021). "Standard test method for rubber property—Durometer hardness," *ASTM International*, West Conshohocken, PA, USA.
- Bassani, A., Montes, S., Jubete, E., Palenzuela, J., Sanjuan, A. P., and Spigno, G. (2019). "Incorporation of waste orange peels extracts into PLA films," *Chemical Engineering*

- Transactions 74, article 1063. DOI: 10.3303/CET1974178
- Bhasney, S. M., Mondal, K., Kumar, A., and Katiyar, V. (2020). "Effect of microcrystalline cellulose [MCC] fibres on the morphological and crystalline behaviour of high density polyethylene [HDPE]/polylactic acid [PLA] blends," *Composites Science and Technology* 187, article 107941. DOI: 10.1016/j.compscitech.2019.107941
- Blanco, I. (2020). "The use of composite materials in 3D printing," *Journal of Composites Science* 4(2), article 42. DOI: 10.3390/jcs4020042
- Cavallo, E., He, X., Luzi, F., Dominici, F., Cerrutti, P., and Bernal, C. (2020). "UV protective, antioxidant, antibacterial and compostable polylactic acid composites containing pristine and chemically modified lignin nanoparticles," *Molecules* 26(1), article 126. DOI: 10.3390/molecules26010126
- Crews, K., Huntley, C., Cooley, D., Phillips, B., and Curry, M. (2016). "Influence of cellulose on the mechanical and thermal stability of ABS plastic composites," *International Journal of Polymer Science* 2016, 1. DOI: 10.1155/2016/9043086
- DeStefano, V., Khan, S., and Tabada, A. (2020). "Applications of PLA in modern medicine," *Engineered Regeneration* 1, 76-87. DOI: 10.1016/j.engreg.2020.08.002
- Estakhrianhaghighi, E., Mirabolghasemi, A., Zhang, Y., Lessard, L., and Akbarzadeh, A. (2020). "3D-printed wood-fiber reinforced architected cellular composites," *Advanced Engineering Materials* 22(11), article 565.DOI: 10.1002/adem.202000565
- Farah, S., Anderson, D. G., and Langer, R. (2016). "Physical and mechanical properties of PLA, and their functions in widespread applications A comprehensive review," *Advanced Drug Delivery Reviews* 107, article 367. DOI: 10.1016/j.addr.2016.06.012
- Guo, N., and Leu, M. C. (2013). "Additive manufacturing: Technology, applications and research needs," *Frontiers of Mechanical Engineering* 8(3), article 215. DOI:10.1007/s11465-013-0248-8
- Huang, S. H., Liu, P., Mokasdar, A., and Hou, L. (2012). "Additive manufacturing and its societal impact: A literature review," *The International Journal of Advanced Manufacturing Technology* 25(13), article 1191. DOI: 10.1007/s00170-012-4558-5
- Ismail, N. R., Fitriyana, N. D. F., Bayuseno, N. a. P., Munanda, N. R., Muhamadin, N. R. C., Nugraha, N. F. W., Rusiyanto, N., Setiyawan, N. A., Bahatmaka, N. A., Firmansyah, N. H. N., Anis, N. S., Irawan, N. a. P., Siregar, N. J. P., and Cionita, N. T.(2023). "Design, manufacturing and characterization of biodegradable bone screw from PLA prepared by fused deposition modelling (FDM) 3D printing technique," *Journal of Advanced Research in Fluid Mechanics and Thermal Sciences* 103(2), 205-215. DOI: 10.37934/arfmts.103.2.205215
- Kalsoom, U., Peristyy, A., Nesterenko, P. N., and Paull, B. (2016). "A 3D printable diamond polymer composite: A novel material for fabrication of low cost thermally conducting devices," *RSC Advances* 6, article 38140-38147. DOI: 10.1039/C6RA05261D
- Kowalczyk, M., Piorkowska, E., Kulpinski, P., and Pracella, M. (2011). "Mechanical and thermal properties of PLA composites with cellulose nanofibers and standard size fibers," *Composites Part A: Applied Science and Manufacturing* 42(10), article 1509. DOI: 10.1016/j.compositesa.2011.07.003
- Krapez Tomec, D., Schöflinger, M., Leßlhumer, J., Gradisar Centa, U., Zigon, J., and Kariz, M. (2024). "The effects of microcrystalline cellulose addition on the properties of wood–PLA filaments for 3D printing," *Polymers* 16(6), article 836. DOI:

- 10.3390/polym16060836
- Kruth, J. P., Leu, M. C., and Nakagawa, T. (1998). "Progress in additive manufacturing and rapid prototyping," *CIRP Annals* 47(2), 525-540. DOI: 10.1016/S0007-8506(07)63240-5
- Lamm, M. E., Wang, L., Kishore, V., Tekinalp, H., Kunc, V., Wang, J., Gardner, D. J., and Ozcan, S. (2020). "Material extrusion additive manufacturing of wood and lignocellulosic filled composites," *Polymers* 12(9), article 2115. DOI: 10.3390/polym12092115
- Lee, J. Y., An, J., and Chua, C. K. (2017). "Fundamentals and applications of 3D printing for novel materials," *Applied Materials Today* 7, article 120. DOI: 10.1016/j.apmt.2017.02.004
- Lupuleasa, D., Draganescu, D., Hincu, L, Tudosa, C. P., and Cioaca, D. (2018). "Biocompatible polymers for 3D printing," *Farmacia* 66, article 737. DOI: 10.31925/Farmacia.2018.5.1
- Moon, R. J., Martini, A., Nairn, J., Simonsen, J., and Youngblood, J. (2011). "Cellulose nanomaterials review: Structure, properties and nanocomposites," *Chemical Society Reviews* 40(7), 3941-3994. DOI: 10.1039/c0cs00108b
- Ngo, T. D., Kashani, A., Imbalzano, G., Nguyen, K. T. Q., and Hui, D. (2018). "Additive manufacturing (3D printing): A review of materials, methods, applications and challenges," *Composites Part B: Engineering* 143, article 172. DOI: 10.1016/j.compositesb.2018.02.012
- Ponsuriyaprakash, S., Udhayakumar, P., and Pandiyarajan, R. (2020). "Experimental investigation of ABS matrix and cellulose fiber reinforced polymer composite materials," *Journal of Natural Fibers* 19(9), article 3241. DOI: 10.1080/15440478.2020.1841065
- Ponsuriyaprakash, S., Udhayakumar, P., Hemalatha, A., and Sabarish, S. (2023). "Additive manufacturing of customized automotive components using novel cellulose fiber reinforced abs polymer filament," *International Journal on Interactive Design and Manufacturing* 17, article 1869. DOI: 10.1007/s12008-023-01316-6
- Qu, P., Gao, Y., Wu, G. F., and Zhang, L. P. (2010). "Nanocomposites of poly(lactic acid) reinforced with cellulose nanofibrils," *BioResources* 5(3), 1811-1823.DOI: 10.15376/biores.5.3.1811-1823
- Raharjo, W. W., Salam, R., and Ariawan, D. (2023). "The effect of microcrystalline cellulose on the physical, thermal, and mechanical properties of composites based on cantala fiber and recycled high-density polyethylene," *Journal of Natural Fibers* 20(2), article 2204454. DOI: 10.1080/15440478.2023.2204454
- Sachin, S. R., Kannan, T. K., and Rajasekar, R. (2020). "Effect of wood particulate size on the mechanical properties of PLA biocomposite," *Pigment & Resin Technology* 49(6), article 465.DOI: 10.1108/PRT-12-2019-0117
- Selwin, M., Rajini, N., Ponsuriyaprakash, S., Ismail S. O., Kumar, K., Faruq, M., Mohammed Rafi, S., and Nadir, A. (2024). "Isolation of microcrystalline cellulose from wood and fabrication of polylactic acid (PLA) based green biocomposites," *Journal of Renewable Materials* 12(8), article 1455. DOI: 10.32604/jrm.2024.052952
- Shao, Y., Guizani, C., Grosseau, P., Chaussy, D., and Beneventi, D. (2018). "Use of ligno cellulosic materials and 3D printing for the development of structured monolithic carbon materials," *Composites Part B: Engineering* 149, article 206. DOI: 10.1016/j.compositesb.2018.05.035

- Singhvi, M. S., Zinjarde, S., and Gokhale, D. (2019). "Polylactic acid: Synthesis and biomedical applications," *Journal of Applied Microbiology* 127, article 1612.DOI: 10.1111/jam.14290
- Velu, R., Raspall, F., and Singamneni, S. (2019). 3D Printing Technologies and Composite Materials for Structural Applications, Elsevier eBooks, 171.
- Wang, X., Jiang, M., Zhou, Z., Gou, J., and Hui, D. (2016). "3D printing of polymer matrix composites: A review and prospective," *Composites Part B: Engineering* 110, article 442. DOI: 10.1016/j.compositesb.2016.11.034
- Wang, C., Yu, J., Jiang, M., and Li, J. (2024). "Effect of selective enhancement on the bending performance of fused deposition methods 3D-printed PLA models," *BioResources* 19(2), 2660-2669. DOI: 10.15376./biores.19.2.2660-2669
- Whyman, S., Arif, K. M., and Potgieter, J. (2018). "Design and development of an extrusion system for 3D printing biopolymer pellets," *The International Journal of Advanced Manufacturing Technology* 96, article 3417.DOI: 10.1007/s00170-018-1843-y
- Yetis, F., Liu, X. Q., Sampson, W. W., and Gong, R. H. (2023). "Biodegradation of composites of polylactic acid and microfibrillated lignocellulose," *Journal of Polymers and the Environment* 31(2), 698-708. DOI: 10.1007/s10924-022-02583-2.

Article submitted: October 26, 2024; Peer review completed: December 2, 2024; Revised version received and accepted: December 17, 2024; Published: August 5, 2025. DOI: 10.15376/biores.20.4.8473-8492